Prospects of Measuring General Higgs Couplings at e^+e^- Linear Colliders

K. Hagiwara[a], S. Ishihara[a,b], J. Kamoshita[c], B.A. Kniehl[d]

[a] Theory Group, KEK,
1-1 Oho, Tsukuba, Ibaraki 305-0801, Japan

[b] Department of Physics, Hyogo University of Education,
941-1 Shimokume, Yashiro, Kato, Hyogo 673-1494, Japan

[c] Department of Physics, Ochanomizu University,
2-1-1 Otsuka, Bunkyo, Tokyo 112-8610, Japan

[d] II. Institut für Theoretische Physik, Universität Hamburg,
Luruper Chaussee 149, 22761 Hamburg, Germany

Abstract

We examine how accurately the general HZV couplings, with $V = Z, \gamma$, may be determined by studying $e^+e^- \to Hf\bar{f}$ processes at future e^+e^- linear colliders. By using the optimal-observable method, which makes use of all available experimental information, we find out which combinations of the various HZV coupling terms may be constrained most efficiently with high luminosity. We also assess the benefits of measuring the tau-lepton helicities, identifying the bottom-hadron charges, polarizing the electron beam and running at two different collider energies. The HZZ couplings are generally found to be well constrained, even without these options, while the $HZ\gamma$ couplings are not. The constraints on the latter may be significantly improved by beam polarization.

1 Introduction

The standard model (SM) of elementary-particle physics predicts a neutral scalar Higgs boson H as a remnant of the spontaneous breaking of its gauge symmetry. This particle is the only undiscovered ingredient of the SM so far. The experiments at the CERN Large Electron-Positron Collider (LEP2) were able to place lower bounds on its mass in the range 91.0–98.8 GeV at the 95% confidence level (CL) [1]. The search for the Higgs boson is a prime target of future colliders. Once the Higgs boson is found, its properties and interactions with other particles may be studied in detail with e^+e^- linear colliders. If the Higgs boson is light, the bremsstrahlung process $e^+e^- \rightarrow HZ$ is expected to be the most promising process to study its properties and interactions and to search for deviations from the SM predictions.

The purpose of this paper is to study systematically the sensitivities to general, non-standard couplings among the Higgs boson, the Z boson and a neutral vector boson V ($V = Z, \gamma$). Since the Z boson has spin one, we take into account the angular distributions of its subsequent decays to fermion-antifermion pairs, in order not to loose information on the interference between amplitudes with different Z-boson helicities. On the other hand, we treat the Higgs boson as a final-state particle because it has spin zero. Thus, we study the production and decay processes

$$e^+e^- \rightarrow HZ; \qquad Z \rightarrow f\bar{f}$$

to obtain sensitivity to general HZV couplings.

We first review previous studies on related problems. The angular distribution of $e^+e^- \rightarrow Hf\bar{f}$ has been analyzed for the SM at the tree level in [2]. Expressions for the cross sections have been elaborated for beam polarization in [3]. Radiative corrections have been investigated in [4]. A comprehensive review of the Higgs boson properties has been given in [5]. The HZZ form factors have been introduced in the study of composite light Higgs bosons [6]. Effects of the non-standard couplings have been discussed in [7, 8]. Z-boson decay angular distribution in the process $e^+e^- \rightarrow HZ$ have been analyzed as a means of distinguishing a scalar form a pseudoscalar Higgs boson in [9].

We employ the optimal-observable method [10, 11, 12, 13] to obtain constraints on the HZV couplings. This method provides the most efficient way to extract physical parameters from experimental data in the sense that the statistical errors on these parameters are minimized. Atwood and Soni have introduced optimal observable quantities in their analysis of electromagnetic form factors of the top quark [10]. The optimal-observable method has also been used in the measurement of the tau polarization [11]. This method has then been extended to the many-parameter case. It has been applied to the determination of the electroweak triple-gauge-boson [12], $Ht\bar{t}$ and HZZ couplings [13].

This paper is organized as follows. In the next section, we cast the differential cross sections of the process $e^+e^- \rightarrow Hf\bar{f}$ into a compact form, to which the optimal-observable method can be applied. We then discuss the properties of the

various terms therein under discrete symmetries. In Sect. 3, we introduce an effective Lagrangian for the HZV interactions and calculate the helicity amplitudes of the process $e^+e^- \to HZ$. In Sect. 4, we determine the achievable errors on the optimal observables introduced in the general expansion of the cross section. In Sect. 5, the optimal constraints on the effective coupling constants are discussed for typical experimental situations. Our conclusions are presented in Sect. 6.

2 Cross section of $e^+e^- \to Hf\bar{f}$

In this section, we present the general angular distributions of the differential cross section of the production and decay process,

$$e^- \left(p_e, \frac{\sigma}{2}\right) + e^+ \left(p_{\bar{e}}, -\frac{\sigma}{2}\right) \to Z^*/\gamma^*(q) \to H(p_H) + Z(p_Z, \lambda), \qquad \text{(2.1-a)}$$

$$Z(p_Z, \lambda) \to f\left(p_f, \frac{\sigma'}{2}\right) + \bar{f}\left(p_{\bar{f}}, -\frac{\sigma'}{2}\right), \qquad \text{(2.1-b)}$$

in a compact form suitable for the optimal-observable method. The four-momentum and helicity of each particle is indicated in parentheses; we have $\sigma = \pm 1$, $\sigma' = \pm 1$ and $\lambda = 0, \pm 1$.

We evaluate the production process (2.1-a) in the centre-of-mass (CM) frame of the colliding beams. The production amplitude is then a function of the scattering angle Θ enclosed between the incoming electron and outgoing Z-boson three-momenta, $\mathbf{p}_e$ and $\mathbf{p}_Z$, respectively. The Z-boson helicity λ is defined in the CM frame of the colliding beams. The y axis is chosen along the $\mathbf{p}_e \times \mathbf{p}_Z$ direction. The decay process (2.1-b) is described in the rest frame of the outgoing Z boson. Here, the z-axis is chosen along the direction of $\mathbf{p}_Z$ (before the boost). The decay amplitude is a function of the polar angle θ and the azimuthal angle φ of the f three-momentum.

2.1 Angular distributions

The angular distributions of the differential cross section of $e^+e^- \to Hf\bar{f}$ may be written as

$$\frac{d\sigma}{d\cos\Theta d\cos\theta d\varphi} = \sum_{i=1}^{9} \left[c_i^{(V)} F_i^{(V)}(\Theta, \theta, \varphi) + c_i^{(A)} F_i^{(A)}(\Theta, \theta, \varphi) \right], \qquad \text{(2.2)}$$

where $c_i^{(V,A)}$ are model-dependent coefficients and $F_i^{(V,A)}$ are known functions of the angles Θ, θ and φ. We shall present the definitions of $c_i^{(V,A)}$ and $F_i^{(V,A)}$ below. The functions $F_i^{(V,A)}$ depend on the flavor of the final-state fermion f and the polarization P of the initial-state electron; we have $P = \pm 1$ if the electron beam is purely

right/left-handed. We assume that the positron beam is unpolarized. In the derivation of $c_i^{(V,A)}$ and $F_i^{(V,A)}$, we use the narrow-width approximation for the Z-boson propagator and the SM amplitude for the decay process $Z \to f\bar{f}$.

We define reduced helicity amplitudes $\hat{M}_\sigma^\lambda$ by extracting the angular dependence from the helicity amplitudes M_σ^λ for $e^+e^- \to HZ$ as

$$M_\sigma^\lambda(e^+e^- \to HZ) = \hat{M}_\sigma^\lambda d_{\sigma,\lambda}^1(\Theta), \tag{2.3}$$

where

$$d_{\sigma,\lambda=0}^1(\Theta) = -\frac{1}{\sqrt{2}}\sigma\sin\Theta, \qquad d_{\sigma,\lambda=\pm}^1(\Theta) = \frac{1}{2}(1+\sigma\lambda\cos\Theta). \tag{2.4}$$

The amplitudes $\hat{M}_\sigma^\lambda$ do not depend on Θ.

The coefficients $c_i^{(V)}$ and $c_i^{(A)}$ are expressed in terms of the amplitudes $\hat{M}_\sigma^\lambda$ as

$$c_1^{(V,A)} = |\hat{M}_R^0|^2 \pm |\hat{M}_L^0|^2, \tag{2.5-a}$$

$$c_2^{(V,A)} = |\hat{M}_R^+|^2 + |\hat{M}_R^-|^2 \pm \left(|\hat{M}_L^+|^2 + |\hat{M}_L^-|^2\right), \tag{2.5-b}$$

$$c_3^{(V,A)} = \mathrm{Re}\left[\hat{M}_R^0(\hat{M}_R^+)^* + \hat{M}_R^-(\hat{M}_R^0)^*\right] \pm \mathrm{Re}\left[\hat{M}_L^0(\hat{M}_L^+)^* + \hat{M}_L^-(\hat{M}_L^0)^*\right], \tag{2.5-c}$$

$$c_4^{(V,A)} = \mathrm{Re}\left[\hat{M}_R^-(\hat{M}_R^+)^*\right] \pm \mathrm{Re}\left[\hat{M}_L^-(\hat{M}_L^+)^*\right], \tag{2.5-d}$$

$$c_5^{(V,A)} = \mathrm{Im}\left[\hat{M}_R^0(\hat{M}_R^+)^* + \hat{M}_R^-(\hat{M}_R^0)^*\right] \pm \mathrm{Im}\left[\hat{M}_L^0(\hat{M}_L^+)^* + \hat{M}_L^-(\hat{M}_L^0)^*\right], \tag{2.5-e}$$

$$c_6^{(V,A)} = \mathrm{Im}\left[\hat{M}_R^-(\hat{M}_R^+)^*\right] \pm \mathrm{Im}\left[\hat{M}_L^-(\hat{M}_L^+)^*\right], \tag{2.5-f}$$

$$c_7^{(V,A)} = |\hat{M}_R^+|^2 - |\hat{M}_R^-|^2 \pm \left(|\hat{M}_L^+|^2 - |\hat{M}_L^-|^2\right), \tag{2.5-g}$$

$$c_8^{(V,A)} = \mathrm{Re}\left[\hat{M}_R^0(\hat{M}_R^+)^* - \hat{M}_R^-(\hat{M}_R^0)^*\right] \pm \mathrm{Re}\left[\hat{M}_L^0(\hat{M}_L^+)^* - \hat{M}_L^-(\hat{M}_L^0)^*\right], \tag{2.5-h}$$

$$c_9^{(V,A)} = \mathrm{Im}\left[\hat{M}_R^0(\hat{M}_R^+)^* - \hat{M}_R^-(\hat{M}_R^0)^*\right] \pm \mathrm{Im}\left[\hat{M}_L^0(\hat{M}_L^+)^* - \hat{M}_L^-(\hat{M}_L^0)^*\right]. \tag{2.5-i}$$

Here, the $+$ $(-)$ sign refers to V (A), and the subscript R (L) stands for $\sigma = +1$ $(\sigma = -1)$. These eighteen coefficients contain all observable consequences of the reduced amplitudes.

The functions $F_i^{(V)}$ are defined as

$$F_1^{(V)} = \frac{r}{4}\sin^2\Theta\sin^2\theta, \tag{2.6-a}$$

$$F_2^{(V)} = \frac{r}{16}(1+\cos^2\Theta)(1+\cos^2\theta) - \frac{rPA_f}{4}\cos\Theta\cos\theta, \tag{2.6-b}$$

$$F_3^{(V)} = -\frac{r}{16}\sin 2\Theta\sin 2\theta\cos\varphi + \frac{rPA_f}{4}\sin\Theta\sin\theta\cos\varphi, \tag{2.6-c}$$

$$F_4^{(V)} = \frac{r}{8}\sin^2\Theta\sin^2\theta\cos 2\varphi, \tag{2.6-d}$$

$$F_5^{(V)} = -\frac{r}{16}\sin 2\Theta\sin 2\theta\sin\varphi + \frac{rPA_f}{4}\sin\Theta\sin\theta\sin\varphi, \tag{2.6-e}$$

4

$$F_6^{(V)} = \frac{r}{8} \sin^2 \Theta \sin^2 \theta \sin 2\varphi, \tag{2.6-f}$$

$$F_7^{(V)} = -\frac{rA_f}{8}(1 + \cos^2 \Theta) \cos \theta + \frac{rP}{8} \cos \Theta (1 + \cos^2 \theta), \tag{2.6-g}$$

$$F_8^{(V)} = \frac{rA_f}{8} \sin 2\Theta \sin \theta \cos \varphi - \frac{rP}{8} \sin \Theta \sin 2\theta \cos \varphi, \tag{2.6-h}$$

$$F_9^{(V)} = \frac{rA_f}{8} \sin 2\Theta \sin \theta \sin \varphi - \frac{rP}{8} \sin \Theta \sin 2\theta \sin \varphi. \tag{2.6-i}$$

The common coefficient r contains some phase space factors and the branching fraction of the $Z \to f\bar{f}$ decay,

$$r = \frac{1}{4} \frac{\beta_{HZ}}{32\pi s} \frac{3}{4\pi} \mathrm{Br}\left(Z \to f\bar{f}\right), \tag{2.7}$$

and A_f is the left-right asymmetry of this decay,

$$A_f = \frac{\left(g_L^f\right)^2 - \left(g_R^f\right)^2}{\left(g_L^f\right)^2 + \left(g_R^f\right)^2}. \tag{2.8}$$

Here, s is the square of the CM energy, and β_{HZ} is the two-body phase-space factor,

$$\beta_{HZ} = \sqrt{1 - 2\frac{m_Z^2 + m_H^2}{s} + \left(\frac{m_Z^2 - m_H^2}{s}\right)^2}. \tag{2.9}$$

The functions $F_i^{(A)}$ are obtained by flipping the P dependence. Specifically, if we write $F_i^{(V)} = \alpha_i + \beta_i P$, with P-independent functions α_i and β_i, then we have $F_i^{(A)} = \alpha_i P + \beta_i$. The explicit expressions read

$$F_1^{(A)} = \frac{rP}{4} \sin^2 \Theta \sin^2 \theta, \tag{2.10-a}$$

$$F_2^{(A)} = \frac{rP}{16}(1 + \cos^2 \Theta)(1 + \cos^2 \theta) - \frac{rA_f}{4} \cos \Theta \cos \theta, \tag{2.10-b}$$

$$F_3^{(A)} = -\frac{rP}{16} \sin 2\Theta \sin 2\theta \cos \varphi + \frac{rA_f}{4} \sin \Theta \sin \theta \cos \varphi, \tag{2.10-c}$$

$$F_4^{(A)} = \frac{rP}{8} \sin^2 \Theta \sin^2 \theta \cos 2\varphi, \tag{2.10-d}$$

$$F_5^{(A)} = -\frac{rP}{16} \sin 2\Theta \sin 2\theta \sin \varphi + \frac{rA_f}{4} \sin \Theta \sin \theta \sin \varphi, \tag{2.10-e}$$

$$F_6^{(A)} = \frac{rP}{8} \sin^2 \Theta \sin^2 \theta \sin 2\varphi, \tag{2.10-f}$$

$$F_7^{(A)} = -\frac{rPA_f}{8}(1 + \cos^2 \Theta) \cos \theta + \frac{r}{8} \cos \Theta (1 + \cos^2 \theta), \tag{2.10-g}$$

$$F_8^{(A)} = \frac{rPA_f}{8} \sin 2\Theta \sin \theta \cos \varphi - \frac{r}{8} \sin \Theta \sin 2\theta \cos \varphi, \tag{2.10-h}$$

$$F_9^{(A)} = \frac{rPA_f}{8} \sin 2\Theta \sin \theta \sin \varphi - \frac{r}{8} \sin \Theta \sin 2\theta \sin \varphi. \tag{2.10-i}$$

The three angular functions $F_1^{(A)}$, $F_4^{(A)}$ and $F_6^{(A)}$ vanish if $P = 0$. One could measure $c_1^{(A)}$, $c_4^{(A)}$ and $c_6^{(A)}$ if $|P| \neq 0$ by combining experiments with opposite polarizations $P = |P|$ and $P = -|P|$.

For most of the hadronic decay modes of the Z boson, the final-state fermions f and $\bar{f}$ cannot be distinguished. Then, we have to average over the configurations with $(\Theta, \theta, \varphi)$ and $(\Theta, \pi - \theta, \varphi \pm \pi)$ as

$$\bar{F}_i^{(V,A)}(\Theta, \theta, \varphi) = \frac{1}{2}\left[F_i^{(V,A)}(\Theta, \theta, \varphi) + F_i^{(V,A)}(\Theta, \pi - \theta, \varphi \pm \pi)\right]. \tag{2.11}$$

This corresponds to setting $A_f = 0$ if f is a quark. If $P = 0$, then one can measure the coefficients $c_1^{(V)}, \ldots, c_6^{(V)}$ and $c_7^{(A)}, \ldots, c_9^{(A)}$, while the coefficients $c_7^{(V)}, \ldots, c_9^{(V)}$ and $c_1^{(A)}, \ldots, c_6^{(A)}$ are only measurable if $P \neq 0$.

When the Z bosons decay to neutrino pairs, one can only measure the Θ distribution, so that the (θ, φ) dependences should be integrated out. Then, we have

$$\frac{d\sigma}{d\cos\Theta} = \sum_{i=1,2,7}\left[c_i^{(V)}\tilde{F}_i^{(V)}(\Theta) + c_i^{(A)}\tilde{F}_i^{(A)}(\Theta)\right], \tag{2.12}$$

where

$$\tilde{F}_1^{(V)} = \frac{2\pi r}{3}\sin^2\Theta, \tag{2.13-a}$$

$$\tilde{F}_2^{(V)} = \frac{\pi r}{3}(1 + \cos^2\Theta), \tag{2.13-b}$$

$$\tilde{F}_7^{(V)} = \frac{2\pi r P}{3}\cos\Theta, \tag{2.13-c}$$

$$\tilde{F}_1^{(A)} = \frac{2\pi r P}{3}\sin^2\Theta, \tag{2.13-d}$$

$$\tilde{F}_2^{(A)} = \frac{\pi r P}{3}(1 + \cos^2\Theta), \tag{2.13-e}$$

$$\tilde{F}_7^{(A)} = \frac{2\pi r}{3}\cos\Theta, \tag{2.13-f}$$

while the other $\tilde{F}_i^{(V,A)}$ functions vanish.

2.2 Discrete symmetries

We now discuss the properties of the $F_i^{(V,A)}$ functions under the discrete symmetries CP and $CP\tilde{T}$. Here, $\tilde{T}$ is the *naive* time reversal symmetry, which flips the momentum and spin of all the particles, but does not reverse the time flow from the initial state to the final state. The non-vanishing of the $CP\tilde{T}$-odd coefficients is related to the presence of absorptive parts in the amplitudes [14].

The electron beam polarization P, the decay asymmetry A_f and the angular variables transform under the discrete symmetries as

$$(P, A_f; \Theta, \theta, \varphi) \overset{CP}{\to} (P, A_f; \pi - \Theta, \pi - \theta, 2\pi - \varphi), \tag{2.14-a}$$

$$(P, A_f; \Theta, \theta, \varphi) \overset{\tilde{T}}{\to} (P, A_f; \Theta, \theta, 2\pi - \varphi). \tag{2.14-b}$$

We can then obtain the symmetry properties of the $F_i^{(V,A)}$ functions, which are summarized in Table 1.

Table 1: CP and $CP\tilde{T}$ properties of the $F_i^{(V,A)}$ functions. A $+$ $(-)$ sign means even (odd) under the symmetry.

i	1	2	3	4	5	6	7	8	9
CP	$+$	$+$	$+$	$+$	$-$	$-$	$-$	$-$	$+$
$CP\tilde{T}$	$+$	$+$	$+$	$+$	$+$	$+$	$-$	$-$	$-$

The coefficients $c_i^{(V,A)}$ have the same symmetry properties as the functions $F_i^{(V,A)}$. The coefficients $c_5^{(V,A)}$ and $c_6^{(V,A)}$ are sensitive to CP-odd and $CP\tilde{T}$-even quantities. When the new-physics effects are generated by exchanges of heavy particles, then the induced vertices should be $CP\tilde{T}$ even. The three $CP\tilde{T}$-odd coefficients $c_7^{(V,A)}$, $c_8^{(V,A)}$ and $c_9^{(V,A)}$ should be proportional to the absorptive parts of the amplitudes which contain light particles in the loops.

3   Helicity amplitudes for $e^+e^- \to HZ$

In this section, we first introduce general couplings and effective form factors for the HZZ and $HZ\gamma$ interactions. We then present the helicity amplitudes of $e^+e^- \to HZ$ using these form factors.

We adopt the effective HZV interaction Lagrangian from [8]. It reads

$$\mathcal{L}_{\text{eff}} = (1 + a_Z)\frac{g_Z m_Z}{2}HZ_\mu Z^\mu + \frac{g_Z}{m_Z}\sum_{V=Z,\gamma}\Big[b_V H Z_{\mu\nu}V^{\mu\nu}$$
$$+ c_V\left(\partial_\mu H Z_\nu - \partial_\nu H Z_\mu\right)V^{\mu\nu} + \tilde{b}_V H Z_{\mu\nu}\tilde{V}^{\mu\nu}\Big], \tag{3.1}$$

where $V_{\mu\nu} = \partial_\mu V_\nu - \partial_\nu V_\mu$ and $\tilde{V}_{\mu\nu} = \epsilon_{\mu\nu\alpha\beta}V^{\alpha\beta}$ with the convention $\epsilon_{0123} = +1$. We have neglected the scalar component of the vector bosons by putting

$$\partial_\mu Z^\mu = \partial_\mu V^\mu = 0. \tag{3.2}$$

Then, the most general parameterization of the HZV interaction involves seven couplings, a_Z, b_Z, c_Z, b_γ, c_γ, $\tilde{b}_Z$ and $\tilde{b}_\gamma$, which are constants as long as we only consider operators through mass dimension five. We note in particular that the operator identity

$$HZ_\mu\partial^2 Z^\mu = HZ_\mu\partial_\nu Z^{\nu\mu}$$
$$= -\frac{1}{2}HZ_{\mu\nu}Z^{\mu\nu} - \frac{1}{2}(\partial_\mu H Z_\nu - \partial_\nu H Z_\mu)Z^{\mu\nu} \tag{3.3}$$

holds under the condition (3.2). The five couplings a_Z, b_Z, c_Z, b_γ and c_γ are CP even, while the remaining two couplings, $\tilde{b}_Z$ and $\tilde{b}_\gamma$, are CP odd. In the effective Lagrangian (3.1), we have factored out the Z-boson coupling g_Z and appropriate powers of m_Z to render the couplings dimensionless. In the SM, we have $a_Z = b_V = c_V = \tilde{b}_V = 0$ at the tree level.

The form factors for the generic $HZ_\alpha V_\beta$ vertex may then be written as

$$\Gamma^V_{\alpha\beta}(q, p_Z) = g_Z m_Z \left[h_1^V(s) g_{\alpha\beta} + \frac{h_2^V(s)}{m_Z^2} q_\alpha p_{Z\beta} + \frac{h_3^V(s)}{m_Z^2} \epsilon_{\alpha\beta\mu\nu} q^\mu p_Z^\nu \right], \qquad (3.4)$$

where the virtual V-boson momentum q is taken to be incoming and the Z-boson momentum p_Z to be outgoing, as depicted in Figure 1 and process (2.1), and $s = q^2$. All form factors h_i^V are dimensionless functions of s. The four form factors h_1^Z, h_2^Z, h_1^γ and h_2^γ are CP even, while the two form factors h_3^Z and h_3^γ are CP odd. It is straightforward to express the form factors in terms of the seven couplings of the effective Lagrangian (3.1):

$$h_1^Z(s) = (1 + a_Z) + 2c_Z \frac{s + m_Z^2}{m_Z^2} + 2(b_Z - c_Z) \frac{s + m_Z^2 - m_H^2}{m_Z^2}, \qquad (3.5\text{-a})$$

$$h_2^Z(s) = -4(b_Z - c_Z), \qquad (3.5\text{-b})$$

$$h_3^Z(s) = -4\tilde{b}_Z, \qquad (3.5\text{-c})$$

$$h_1^\gamma(s) = 2c_\gamma \frac{s}{m_Z^2} + (b_\gamma - c_\gamma) \frac{s + m_Z^2 - m_H^2}{m_Z^2}, \qquad (3.5\text{-d})$$

$$h_2^\gamma(s) = -2(b_\gamma - c_\gamma), \qquad (3.5\text{-e})$$

$$h_3^\gamma(s) = -2\tilde{b}_\gamma. \qquad (3.5\text{-f})$$

Although the effective Lagrangian has seven couplings, there are only six form factors. Thus, one combination of couplings cannot be measured at one given collider energy. Details will be discussed in Sect. 5.

We now evaluate the helicity amplitudes $M_\sigma^\lambda(e^+ e^- \to HZ)$ for the production process. After extracting the angular dependence according to (2.3), we obtain the reduced amplitudes[1] as functions of s:

$$\hat{M}_\sigma^{\lambda=0}(s) = -g_Z^2 g_\sigma^e \sqrt{2s} E_Z D_Z(s) \left(h_1^Z + h_2^Z \frac{\sqrt{s} E_Z \beta_Z^2}{m_Z^2} \right)$$

$$+ eg_Z \sqrt{2s} E_Z D_\gamma(s) \left(h_1^\gamma + h_2^\gamma \frac{\sqrt{s} E_Z \beta_Z^2}{m_Z^2} \right), \qquad (3.6\text{-a})$$

$$\hat{M}_\sigma^{\lambda=\pm}(s) = -g_Z^2 g_\sigma^e \sqrt{2s} m_Z D_Z(s) \left(h_1^Z + i\lambda h_3^Z \frac{\sqrt{s} E_Z \beta_Z}{m_Z^2} \right)$$

$$+ eg_Z \sqrt{2s} m_Z D_\gamma(s) \left(h_1^\gamma + i\lambda h_3^\gamma \frac{\sqrt{s} E_Z \beta_Z}{m_Z^2} \right). \qquad (3.6\text{-b})$$

---

[1] In [8], there is a misprint in the relative sign of the helicity amplitudes. There should be an overall minus sign on the right-hand side of (2.3) therein. Furthermore, $\text{Im}\,[(\hat{M}_\sigma^+ + \hat{M}_\sigma^-)(\hat{M}_\sigma^0)^*]$ and $\text{Im}\,[(\hat{M}_\sigma^+ - \hat{M}_\sigma^-)(\hat{M}_\sigma^0)^*]$ should be interchanged in the first column of Table 1.

where $g_R^e = \sin^2 \theta_W$, $g_L^e = -1/2 + \sin^2 \theta_W$, $\beta_Z = \sqrt{1 - m_Z^2/E_Z^2}$ and

$$D_Z(s) = \frac{1}{s - m_Z^2 + i m_Z \Gamma_Z}, \tag{3.7}$$

$$D_\gamma(s) = \frac{1}{s}. \tag{3.8}$$

The energy of the outgoing Z boson is

$$E_Z = \frac{\sqrt{s}}{2}\left(1 - \frac{m_H^2 - m_Z^2}{s}\right). \tag{3.9}$$

The couplings g_R^e and g_L^e have almost the same magnitudes, but their signs are opposite to each other. Thus, the coefficients $c_i^{(V)}$ are sensitive to the HZZ couplings, while the coefficients $c_i^{(A)}$ are sensitive to the $HZ\gamma$ couplings.

4   Optimal observables

We now employ the optimal-observable method [12, 13] to obtain the errors on the coefficients $c_i^{(V)}$ and $c_i^{(A)}$. In order to simplify the notation, let us re-sequence the coefficients and functions for the time being as

$$(c_1, \ldots, c_{18}) = (c_1^{(V)}, \ldots, c_9^{(V)}, c_1^{(A)}, \ldots, c_9^{(A)}), \tag{4.1-a}$$

$$(F_1, \ldots, F_{18}) = (F_1^{(V)}, \ldots, F_9^{(V)}, F_1^{(A)}, \ldots, F_9^{(A)}). \tag{4.1-b}$$

According to the optimal-observable method, the covariance matrix V_{ij} for the coefficients c_i is given by

$$V_{ij}^{-1} = L \int \frac{F_i(\Theta, \theta, \varphi) F_i(\Theta, \theta, \varphi)}{\Sigma_{\mathrm{SM}}(\Theta, \theta, \varphi)} d\cos\Theta \cos\theta d\varphi, \tag{4.2}$$

where L is the integrated luminosity of the experiment and

$$\Sigma_{\mathrm{SM}}(\Theta, \theta, \varphi) = \frac{d\sigma_{\mathrm{SM}}}{d\cos\Theta \cos\theta d\varphi}(\Theta, \theta, \varphi). \tag{4.3}$$

The statistical error on c_i is $\sqrt{V_{ii}}$, and the correlation between the error on c_i and that on c_j is $V_{ij}/\sqrt{V_{ii}V_{jj}}$. We use this method to obtain V_{ij}^{-1} for each decay mode of the Z boson. We then combine these results for all the Z-boson decay modes.

The differential cross section Σ_{SM} is a linear combination of $F_1^{(V)}, \ldots, F_4^{(V)}$ and $F_1^{(A)}, \ldots, F_4^{(A)}$, which are CP and $CP\tilde{T}$ even. The component V_{ij} of the covariance matrix vanishes if F_i and F_j have different CP or $CP\tilde{T}$ properties. Thus, the covariance matrix is block diagonalized into four sub-matrices according to the CP and $CP\tilde{T}$ properties of the F_i functions discussed in Sect. 2.2. Notice that this

9

argument is only valid if we integrate in (4.2) over the full angle domains. In practice, there are excluded regions due to the geometry of the detectors or cuts for selecting events. Thus, the block diagonal structure of the covariance matrix is only approximately realized in practice. In the present study, we shall integrate over the full phase space.

We estimate how the optimal errors are reduced by the following three additional techniques. The first one is the tau helicity measurement. We adopt $\epsilon_\tau = 40\%$ as the efficiency factor to determine the helicities of the decaying τ^+ or τ^- leptons. The second technique is the electric-charge identification for the bottom quarks and antiquarks. The charge of a hadron B containing one b or $\bar{b}$ quark can be identified via the decay mode $B \to l\nu + X$. We assume an efficiency of $\epsilon_b = 20\%$ for identifying the charges of the decaying b or $\bar{b}$ hadrons. The third technique is to employ electron beam polarization P. We take $|P| = 90\%$ as the target polarization. Specifically, we assume that one half of the beam is polarized with $P = 0.9$ and the other half with $P = -0.9$.

For the fraction ϵ_τ of the $Z \to \tau^+\tau^-$ decays, one can distinguish the tau polarization. In order to assess the possible benefits of the tau polarization measurement, we make the simple assumption that the efficiency for observing a left- or right-handed tau lepton is ϵ_τ. Then, we substitute in (2.6) and (2.10)

$$r = \frac{3\beta_{HZ}}{512\pi^2 s}\mathrm{Br}(Z \to \tau^+\tau^-)\frac{\left(g^\tau_{L/R}\right)^2}{\left(g^\tau_L\right)^2 + \left(g^\tau_R\right)^2}\epsilon_\tau, \tag{4.4-a}$$

$$A_f = \pm 1 \tag{4.4-b}$$

for left/right-handed tau leptons. In actual experiments, one should not only estimate the efficiency factor ϵ_τ for each pair of τ^+ and τ^- decay modes, but also a correlation between the constraints from τ^-_R production and those from τ^-_L production. We return to this problem at the end of this section.

Throughout our numerical analysis, we set $m_Z = 91.187$ GeV [15], $\alpha = 1/128.9$ [16], $\sin^2\theta_W = 0.2312$ and $g_Z = \sqrt{4\sqrt{2}G_F m_Z^2} = 0.74070$. As an example, we show results for the Higgs boson mass $m_H = 120$ GeV, the CM energy $\sqrt{s} = 250$ GeV and the nominal integrated luminosity $L = 10$ fb^{-1}.

We first present the results for $\epsilon_\tau = \epsilon_b = P = 0$. The results for the CP-even and $CP\tilde{T}$-even coefficients and their block in the covariance matrix are

$$
\begin{aligned}
c_1^{(V)} &= .0208 \pm .0011 \\
c_2^{(V)} &= .0271 \pm .0012 \\
c_3^{(V)} &= .0336 \pm .0049 \\
c_4^{(V)} &= .0136 \pm .0026 \\
c_2^{(A)} &= -.004 \pm .025 \\
c_3^{(A)} &= -.005 \pm .020
\end{aligned}
\quad
\begin{pmatrix}
1 & & & & & \\
-.66 & 1 & & & & \\
-.02 & .13 & 1 & & & \\
.10 & -.02 & .06 & 1 & & \\
.00 & -.00 & -.00 & -.00 & 1 & \\
-.00 & -.00 & -.00 & -.00 & .10 & 1
\end{pmatrix}.
\tag{4.5}
$$

The results for the CP-odd and $CP\tilde{T}$-even coefficients are

$$
\begin{array}{cc}
c_5^{(V)} = 0 \pm .0047 \\
c_6^{(V)} = 0 \pm .0026, \\
c_5^{(A)} = 0 \pm .018
\end{array}
\qquad
\begin{pmatrix}
1 & & \\
.07 & 1 & \\
-.00 & -.00 & 1
\end{pmatrix}.
\tag{4.6}
$$

The results for the CP-odd and $CP\tilde{T}$-odd coefficients are

$$
\begin{array}{cc}
c_7^{(V)} = 0 \pm .021 \\
c_8^{(V)} = 0 \pm .042 \\
c_7^{(A)} = 0 \pm .0010, \\
c_8^{(A)} = 0 \pm .0022
\end{array}
\qquad
\begin{pmatrix}
1 & & & \\
.12 & 1 & & \\
-.00 & -.00 & 1 & \\
-.00 & -.00 & .11 & 1
\end{pmatrix}.
\tag{4.7}
$$

The results for the CP-even and $CP\tilde{T}$-odd coefficients are

$$
\begin{array}{cc}
c_9^{(V)} = 0 \pm .039 \\
c_9^{(A)} = 0 \pm .0021,
\end{array}
\qquad
\begin{pmatrix}
1 & \\
-.00 & 1
\end{pmatrix}.
\tag{4.8}
$$

There are no constraints on $c_1^{(A)}$, $c_4^{(A)}$ and $c_6^{(A)}$ because $F_1^{(A)}$, $F_4^{(A)}$ and $F_6^{(A)}$ vanish if $P = 0$. The errors on $c_2^{(A)}$, $c_3^{(A)}$, $c_5^{(A)}$, $c_7^{(V)}$, $c_8^{(V)}$ and $c_9^{(V)}$ are relatively large because the corresponding $F_i^{(V,A)}$ functions in (2.10) are suppressed by the smallness of A_f and the vanishing of P.

Next, we present the results for $\epsilon_\tau = 40\%$, $\epsilon_b = 20\%$ and $|P| = 90\%$. The results for the CP-even and $CP\tilde{T}$-even coefficients are

$$
\begin{array}{cc}
c_1^{(V)} = .0208 \pm .0011 \\
c_2^{(V)} = .0271 \pm .0012 \\
c_3^{(V)} = .0336 \pm .0028 \\
c_4^{(V)} = .0136 \pm .0026 \\
c_1^{(A)} = -.0031 \pm .0012, \\
c_2^{(A)} = -.0041 \pm .0013 \\
c_3^{(A)} = -.0050 \pm .0027 \\
c_4^{(A)} = -.0020 \pm .0029
\end{array}
\qquad
\begin{pmatrix}
1 & & & & & & & \\
-.65 & 1 & & & & & & \\
.14 & .06 & 1 & & & & & \\
.10 & -.01 & .20 & 1 & & & & \\
-.13 & .08 & -.03 & -.01 & 1 & & & \\
.08 & -.13 & .00 & -.00 & -.65 & 1 & & \\
-.03 & .00 & -.06 & -.04 & .15 & .05 & 1 & \\
-.01 & -.00 & -.04 & -.13 & .10 & -.01 & .20 & 1
\end{pmatrix}.
\tag{4.9}
$$

The results for the CP-odd and $CP\tilde{T}$-even coefficients are

$$
\begin{array}{cc}
c_5^{(V)} = 0 \pm .0031 \\
c_6^{(V)} = 0 \pm .0026 \\
c_5^{(A)} = 0 \pm .0030, \\
c_6^{(A)} = 0 \pm .0029
\end{array}
\qquad
\begin{pmatrix}
1 & & & \\
.18 & 1 & & \\
-.11 & -.04 & 1 & \\
-.03 & -.13 & .19 & 1
\end{pmatrix}.
\tag{4.10}
$$

The results for the CP-odd and $CP\tilde{T}$-odd coefficients are

$$
\begin{array}{cc}
c_7^{(V)} = 0 \pm .0011 \\
c_8^{(V)} = 0 \pm .0023 \\
c_7^{(A)} = 0 \pm .0010, \\
c_8^{(A)} = 0 \pm .0021
\end{array}
\qquad
\begin{pmatrix}
1 & & & \\
.17 & 1 & & \\
-.13 & -.03 & 1 & \\
-.03 & -.12 & .16 & 1
\end{pmatrix}.
\tag{4.11}
$$

11

The results for the CP-even and $CP\tilde{T}$-odd coefficients are

$$
\begin{aligned}
c_9^{(V)} &= 0 \pm .0023 \\
c_9^{(A)} &= 0 \pm .0021
\end{aligned}
, \qquad
\begin{pmatrix} 1 & \\ -.13 & 1 \end{pmatrix}.
\tag{4.12}
$$

The errors on $c_i^{(A)}$ with $i = 1, \ldots, 6$ and $c_i^{(V)}$ with $i = 7, 8, 9$ are reduced to the level of those on the other coefficients because the suppression of the corresponding $F_i^{(V,A)}$ functions in (2.10) is weaker than in the case of $\epsilon_\tau = \epsilon_b = P = 0$. On the other hand, the errors on the other coefficients are not further reduced relative to the former situation.

We mention here the effect of the correlation between the constraints from τ_R production and those from τ_L production. In actual experiments, τ_L and τ_R leptons can only be identified on a statistical basis. The analyzing power of the semileptonic tau decays is, in principle, equal for all the semileptonic tau decay modes [17]. By using the $\tau^- \to \nu_\tau \pi^-$ decay mode, we evaluate the effect of the τ_L-τ_R correlation on the errors on $c_i^{(V,A)}$. We find that the errors on $c_i^{(V,A)}$ may be increased by about 20% in actual experiments.

5 Constraints on general HZV couplings

We are now ready to study the sensitivities to the seven general HZV coupling constants. The errors on these couplings are obtained from those on $c_i^{(V,A)}$ by using (2.5), (3.5) and (3.6). We quantitatively analyze the usefulness of electron beam polarization and of an additional experiment with another beam energy. For consistency of the analysis that includes the operators through mass dimension five, we only keep in $c_i^{(V,A)}$ terms linear in the coupling.

5.1 Real part

We first discuss the constraints on the real parts of the general HZV couplings. The constraints on the real parts of the CP-even couplings are obtained from the CP-even and $CP\tilde{T}$-even coefficients $c_1^{(V,A)}, \ldots, c_4^{(V,A)}$, while those on the real parts of the CP-odd couplings are obtained from the CP-odd and $CP\tilde{T}$-even coefficients $c_5^{(V,A)}$ and $c_6^{(V,A)}$.

We first present the results for $\sqrt{s} = 250$ GeV. The optimal errors on the HZV couplings are summarized in Table 2. We only gain sensitivity to six combinations of couplings. As long as we consider experiments at a fixed collider energy, one combination of couplings cannot be measured. The unmeasurable combination of couplings is determined from (3.5) and reads

$$
a_Z - (b_Z + c_Z)\frac{m_Z^2}{2(s + m_Z^2)}.
\tag{5.1}
$$

Table 2: Optimal errors on the real parts of the general HZV couplings at $\sqrt{s} = 250$ GeV.

ϵ_τ	—	0.4	—	—	0.4
ϵ_b	—	—	0.2	—	0.2
$\|P\|$	—	—	—	0.9	0.9
$\mathrm{Re}\,(b_Z + .059a_Z)$	.0061	.0036	.0033	.0030	.0029
$\mathrm{Re}\,(c_Z + .059a_Z)$	.013	.0076	.0070	.0061	.0061
$\mathrm{Re}\,b_\gamma$	.19	.072	.053	.0085	.0084
$\mathrm{Re}\,c_\gamma$	.12	.047	.035	.0053	.0052
$\mathrm{Re}\,\tilde{b}_Z$	.012	.011	.010	.010	.0091
$\mathrm{Re}\,\tilde{b}_\gamma$	.094	.036	.026	.016	.013

It is independent of the final-state fermion flavour f and the electron beam polarization P. We are thus insensitive to this combination for all Z-bosons decay modes. Since a_Z is the dominant part of (5.1), we fix a_Z to obtain the optimal sensitivities to the remaining six coupling constants b_Z, c_Z, b_γ, c_γ, $\tilde{b}_Z$ and $\tilde{b}_\gamma$. The combinations $\mathrm{Re}\,(b_Z + .059a_Z)$ and $\mathrm{Re}\,(c_Z + .059a_Z)$, which appear in Table 2, are orthogonal to the unmeasurable combination (5.1).

For $\epsilon_\tau = \epsilon_b = P = 0$, we have good sensitivities only to the three HZZ couplings b_Z, c_Z and $\tilde{b}_Z$, but not to the $HZ\gamma$ couplings b_γ, c_γ and $\tilde{b}_\gamma$, which is evident from Table 2. The functions $F_i^{(A)}$ with $i = 1, \ldots, 6$ are suppressed in magnitude by the smallness of A_f and the vanishing of P, while the functions $F_i^{(V)}$ with $i = 1, \ldots, 6$ have unsuppressed parts.

By using any of the three additional techniques, we gain better sensitivities to the $HZ\gamma$ couplings because $F_i^{(A)}$ with $i = 1, \ldots, 6$ are then less suppressed. The measurement of the tau helicity with 40% efficiency reduces the errors on b_γ, c_γ and $\tilde{b}_\gamma$ by a factor of about $2/5$ relative to the case without tau helicity measurement. Bottom charge identification with 20% efficiency reduces the errors on these couplings by a factor of $2/7$. We observe that the tau helicity measurement leads to an improvement comparable to that for the bottom charge identification. This may be understood qualitatively from the relation

$$\sqrt{\frac{\epsilon_b}{\epsilon_\tau} \frac{\mathrm{Br}(Z \to b\bar{b})}{\mathrm{Br}(Z \to \tau^-\tau^+)}}|A_b| \approx 1.5 \approx \frac{2/5}{2/7}. \tag{5.2}$$

The electron beam polarization is the most efficient technique for improving the sensitivities. It reduces the errors on the CP-even (CP-odd) $HZ\gamma$ couplings by a factor of about $1/20$ ($1/6$). A qualitative understanding hereof is obtained from the

relation

$$\sqrt{\frac{1}{\epsilon_\tau} \frac{1}{\mathrm{Br}(Z \to \tau^- \tau^+)}} |P| \approx 8.2 \approx \frac{2/5}{1/20}, \tag{5.3}$$

for the CP-even couplings. We find from Table 2 that the errors on the CP-even HZZ couplings are reduced by a factor of $1/2$ with these three additional techniques, while the CP-odd HZZ couplings are almost unchanged.

For $\epsilon_\tau = \epsilon_b = P = 0$, the errors on the real parts of the couplings and the corresponding correlation matrix are

$$
\begin{aligned}
\mathrm{Re}\,(b_Z + .059 a_Z) &= 0 \pm .0061 \\
\mathrm{Re}\,(c_Z + .059 a_Z) &= 0 \pm .013 \\
\mathrm{Re}\,b_\gamma &= 0 \pm .19 \\
\mathrm{Re}\,c_\gamma &= 0 \pm .12 \\
\mathrm{Re}\,\tilde{b}_Z &= 0 \pm .012 \\
\mathrm{Re}\,\tilde{b}_\gamma &= 0 \pm .094
\end{aligned}
\quad ,
\begin{pmatrix}
1 & & & & & \\
-.95 & 1 & & & & \\
-.86 & .88 & 1 & & & \\
.83 & -.89 & -.99 & 1 & & \\
0 & 0 & 0 & 0 & 1 & \\
0 & 0 & 0 & 0 & -.46 & 1
\end{pmatrix}. \tag{5.4}
$$

There are strong correlations among the errors on b_Z, c_Z, b_γ and c_γ. Thus, a certain combination of parameters is more strongly constrained than the individual parameters. The eigenvector with the smallest eigenvalue and its error read

$$\mathrm{Re}\,(.08 a_Z + .90 b_Z + .42 c_Z + .05 b_\gamma + .08 c_\gamma) = 0 \pm .00076. \tag{5.5}$$

The above combination may be understood qualitatively by observing that an experiment at $\sqrt{s} = 250$ GeV operates near the threshold of the HZ production process, where $\beta_{HZ} \approx 0$. Near the threshold, the form factors h_1^Z and h_1^γ play a dominant role in the helicity amplitudes, while the residual form factors are suppressed by the smallness of β_{HZ}. Specifically, we have

$$\hat{M}_\sigma^\lambda = g_Z \sqrt{2s} m_Z \left[-g_Z g_\sigma^e D_Z(s) h_1^Z + e D_\gamma(s) h_1^\gamma \right] + O(\beta). \tag{5.6}$$

Furthermore, the sensitivities to the $HZ\gamma$ couplings are diminished for $\epsilon_\tau = \epsilon_b = P = 0$ because $\sin^2 \theta_W \approx 1/4$. Thus, near threshold there is good sensitivity to the following combination of couplings:

$$h_1^Z \approx 1 + a_Z + 4 b_Z \left(1 + \frac{m_H}{m_Z} \right) + 2 c_Z \frac{m_H^2}{m_Z^2}. \tag{5.7}$$

This is essentially the combination that appears in the constraint (5.5).

In models with multiple Higgs doublets, including the minimal supersymmetric extension of the SM (MSSM), the coupling a_Z is modified at the tree level, while the couplings b_V, c_V and $\tilde{b}_V$ only receive corrections at the loop level. Thus, we discuss here the sensitivity to a_Z when $b_V = c_V = \tilde{b}_V = 0$. From (5.4), we obtain at $\sqrt{s} = 250$ GeV

$$a_Z = 0 \pm 0.010 \tag{5.8}$$

if $b_V = c_V = 0$.

For $\epsilon_\tau = 40\%$, $\epsilon_b = 20\%$ and $|P| = 90\%$, the errors and correlation matrix are found to be

$$
\begin{array}{ll}
\mathrm{Re}\,(b_Z + .059 a_Z) = 0 \pm .0029 \\
\mathrm{Re}\,(c_Z + .059 a_Z) = 0 \pm .0061 \\
\mathrm{Re}\,b_\gamma \qquad\quad = 0 \pm .0084 \\
\mathrm{Re}\,c_\gamma \qquad\quad = 0 \pm .0052 \\
\mathrm{Re}\,\tilde{b}_Z \qquad\quad = 0 \pm .0091 \\
\mathrm{Re}\,\tilde{b}_\gamma \qquad\quad = 0 \pm .013
\end{array}
\qquad
\left(
\begin{array}{cccccc}
1 & & & & & \\
-.96 & 1 & & & & \\
-.08 & .08 & 1 & & & \\
.08 & -.09 & -.99 & 1 & & \\
0 & 0 & 0 & 0 & 1 & \\
0 & 0 & 0 & 0 & -.09 & 1
\end{array}
\right).
\qquad (5.9)
$$

We obtain similar correlation matrices for the other situations when only one of the three additional measurements is employed. The correlations between the HZZ and $HZ\gamma$ couplings then disappear. There are still strong correlations between b_Z and c_Z and between b_γ and c_γ. The eigenvectors of the two smallest eigenvalues and their errors are

$$
\mathrm{Re}\,(.025 a_Z + .28 b_Z + .14 c_Z + .50 b_\gamma + .81 c_\gamma) = 0 \pm .00068, \qquad (5.10\text{-a})
$$
$$
\mathrm{Re}\,(.074 a_Z + .86 b_Z + .40 c_Z - .17 b_\gamma - .27 c_\gamma) = 0 \pm .00078. \qquad (5.10\text{-b})
$$

As in (5.6), the form factors h_1^Z and h_1^γ become dominant near the threshold, and there is good sensitivity to the following two combinations of couplings:

$$
h_1^Z \approx 1 + a_Z + 4 b_Z \left(1 + \frac{m_H}{m_Z}\right) + 2 c_Z \frac{m_H^2}{m_Z^2}, \qquad (5.11\text{-a})
$$

$$
h_1^\gamma \approx 2 b_\gamma \left(1 + \frac{m_H}{m_Z}\right) + 2 c_\gamma \left(\frac{m_H}{m_Z} + \frac{m_H^2}{m_Z^2}\right). \qquad (5.11\text{-b})
$$

The most-strongly constrained combinations listed in (5.10) are essentially linear superpositions of $h_1^Z - 1$ and h_1^γ as given in (5.11).

We now discuss the sensitivity to a_Z when $b_V = c_V = \tilde{b}_V = 0$. The six-parameter constraints (5.9) then lead to the one-parameter constraint

$$
a_Z = 0 \pm 0.010 \qquad (5.12)
$$

at $\sqrt{s} = 250$ GeV. This constraint is same as in (5.8). The error on a_Z is not diminished by any of the three experimental options.

Figure 2 displays the contours of $\chi^2 = 1$ (39% CL) in the (b_γ, c_γ) plane for the different modes of experiment. The other five degrees of couplings have been integrated out. We observe that there is a strong correlation between b_γ and c_γ for all experimental methods. As mentioned above, the specific combination of b_γ and c_γ contained in (5.10) is thus tightly restricted. We can see from Figure 2 that the individual sensitivities to b_γ and c_γ are drastically improved by the electron beam polarization. This means that we can obtain strict constrains on any model that predicts large $HZ\gamma$ couplings by using data from experiments with polarized electron beams.

Figure 3 displays the contours of $\chi^2 = 1$ in the (b_Z, c_Z) plane. We see that the HZZ couplings are well constrained even if $\epsilon_\tau = \epsilon_b = P = 0$. The three charge and polarization measurements lead to moderate reductions of the errors on b_Z and c_Z.

Figure 4 shows the contours of $\chi^2 = 1$ in the $(\tilde{b}_Z, \tilde{b}_\gamma)$ plane. The three charge and polarization measurements mainly reduce the error on $\tilde{b}_\gamma$. The reduction of the error on $\tilde{b}_\gamma$ is transferred to that on $\tilde{b}_Z$ via the correlation between $\tilde{b}_Z$ and $\tilde{b}_\gamma$.

Next, we consider the case of $\sqrt{s} = 500$ GeV. The results for $\epsilon_\tau = 40\%$, $\epsilon_b = 20\%$ and $P = 90\%$ are

$$
\begin{array}{ll}
\text{Re}\,(b_Z + .016a_Z) = 0 \pm .0015 \\
\text{Re}\,(c_Z + .016a_Z) = 0 \pm .0007 \\
\quad\text{Re}\,b_\gamma \quad\quad = 0 \pm .0024 \\
\quad\text{Re}\,c_\gamma \quad\quad = 0 \pm .0005 \\
\quad\text{Re}\,\tilde{b}_Z \quad\quad = 0 \pm .0042 \\
\quad\text{Re}\,\tilde{b}_\gamma \quad\quad = 0 \pm .0052
\end{array}
\qquad
\left(
\begin{array}{cccccc}
1 \\
-.77 & 1 \\
-.09 & .07 & 1 \\
.07 & -.09 & -.84 & 1 \\
0 & 0 & 0 & 0 & 1 \\
0 & 0 & 0 & 0 & -.09 & 1
\end{array}
\right).
\qquad (5.13)
$$

Although the cross section at $\sqrt{s} = 500$ GeV is smaller the one at $\sqrt{s} = 250$ GeV, the errors are reduced because b_V, c_V and $\tilde{b}_V$ are accompanied by a factor of s/m_Z^2. Increasing the CM energy from $\sqrt{s} = 250$ GeV to $\sqrt{s} = 500$ GeV reduces the errors on b_Z and b_γ by a factor of $1/2$ to $1/3$ and those on c_Z and c_γ by a factor of $1/7$ to $1/10$. This also reduces the errors on the CP-odd couplings $\tilde{b}_Z$ and $\tilde{b}_\gamma$ by a factor of $1/2$. The strong correlations are lost because the experiment at $\sqrt{s} = 500$ GeV is far above the threshold, and the various form factors in the helicity amplitudes are non-negligible. At $\sqrt{s} = 500$ GeV, the sensitivity to a_Z becomes

$$
a_Z = 0 \pm 0.021 \qquad (5.14)
$$

if b_V, c_V and $\tilde{b}_V$ are fixed to zero. This error is larger than the one at $\sqrt{s} = 250$ GeV because a_Z is the coefficient of the renormalizable dimension-four operator. We conclude that a_Z may be well measured at the CM energy where the cross section of HZ production has its maximum.

Finally, we present optimal constraints on the seven parameters in (3.1) by combining the analyses at $\sqrt{s} = 250$ GeV and $\sqrt{s} = 500$ GeV with $\epsilon_\tau = 40\%$, $\epsilon_b = 20\%$ and $P = 90\%$. Here, we face the problem that our results depend on the integrated luminosities at the two energies. At fixed energy, our constraints scale as $L^{-1/2}$. We can arbitrarily scale our results by changing the nominal value of L, which could include more realistic experimental efficiencies. Once we combine the analyses at the two energies, our results will depend on the ratio of the two respective values of L, which we cannot fix a priori. For simplicity, we assume the same luminosity,

$L = 10 \text{ fb}^{-1}$, at both energies. The results are then

$$
\begin{aligned}
\mathrm{Re}\,(b_Z + .066a_Z) &= 0 \pm .0009 \\
\mathrm{Re}\,c_Z &= 0 \pm .0006 \\
\mathrm{Re}\,b_\gamma &= 0 \pm .0015 \\
\mathrm{Re}\,c_\gamma &= 0 \pm .0004 \\
\mathrm{Re}\,\tilde{b}_Z &= 0 \pm .0038 \\
\mathrm{Re}\,\tilde{b}_\gamma &= 0 \pm .0049
\end{aligned}
\qquad
\begin{pmatrix}
1 & & & & & \\
-.68 & 1 & & & & \\
-.08 & .07 & 1 & & & \\
.06 & -.08 & -.79 & 1 & & \\
0 & 0 & 0 & 0 & 1 & \\
0 & 0 & 0 & 0 & -.09 & 1
\end{pmatrix}.
\tag{5.15}
$$

The minimum χ^2 is found to be

$$
\chi^2_{\min} = \left(\frac{a_Z}{0.024}\right)^2.
\tag{5.16}
$$

So far, we have considered a_Z as a fixed parameter. Now, $\chi^2_{\min}$ is a function of a_Z, so that we can obtain optimal constraints on all seven HZV couplings. The result is

$$
\begin{aligned}
\mathrm{Re}\,a_Z &= 0 \pm .024 \\
\mathrm{Re}\,b_Z &= 0 \pm .0018 \\
\mathrm{Re}\,c_Z &= 0 \pm .0006 \\
\mathrm{Re}\,b_\gamma &= 0 \pm .0015 \\
\mathrm{Re}\,c_\gamma &= 0 \pm .0004 \\
\mathrm{Re}\,\tilde{b}_Z &= 0 \pm .0038 \\
\mathrm{Re}\,\tilde{b}_\gamma &= 0 \pm .0049
\end{aligned}
\qquad
\begin{pmatrix}
1 & & & & & & \\
-.87 & 1 & & & & & \\
-.02 & -.31 & 1 & & & & \\
.00 & -.04 & .07 & 1 & & & \\
.00 & .03 & -.08 & -.79 & 1 & & \\
0 & 0 & 0 & 0 & 0 & 1 & \\
0 & 0 & 0 & 0 & 0 & -.09 & 1
\end{pmatrix}.
\tag{5.17}
$$

Now, a_Z is weakly constrained. There is a strong correlation between a_Z and b_Z. This reflects the fact that the combination $\mathrm{Re}\,(b_Z + .066a_Z)$ in (5.15) is more strongly constrained than $\mathrm{Re}\,b_Z$.

Figure 5 illustrates how a_Z is constrained. As mentioned above, there is a combination of couplings, namely the one in (5.1), that is not constrained by an experiment at a single CM energy. The projections of the cylinder defined by $\chi^2 = 1$ onto the (a_Z, b_Z), (b_Z, c_Z) and (c_Z, a_Z) planes are indicated as the stripes between the dashed (thin solid) lines for $\sqrt{s} = 250$ (500) GeV. Because the direction of the cylinder varies with $\sqrt{s}$, the measurements at the two energies, $\sqrt{s} = 250$ GeV and 500 GeV, lead to individual constraints on a_Z, b_Z and c_Z.

So far, we have assumed that a_Z is constant. In general, a_Z may have some energy dependence,

$$
a_Z(s) = a_Z(0) + s a'_Z(0) + O(s^2).
\tag{5.18}
$$

The $O(s^2)$ term is neglected in our approximation. In terms of operators, the derivative term corresponds to a dimension-five operator and should be exhausted by the effective Lagrangian (3.1). In fact, it may be written as a linear combination of the b_Z and c_Z terms because of the operator identity (3.3).

5.2 Imaginary part

We now discuss the sensitivities to the imaginary parts of the general HZV couplings. Imaginary parts can arise if the couplings are induced by new interactions involving particles that can be produced at the energy of the considered experiment. For consistency, we neglect the absorptive part in the Z-boson propagator as we ignore all absorptive parts in the SM amplitudes. The constraints on the imaginary parts of the CP-even couplings are then obtained from the CP-even and $CP\tilde{T}$-odd coefficient $c_9^{(V,A)}$, while the constraints on the imaginary parts of the CP-odd couplings are obtained from the CP-odd and $CP\tilde{T}$-odd coefficients $c_7^{(V,A)}$ and $c_8^{(V,A)}$. The results are summarized in Table 3. In contrast to the real parts of the HZV

Table 3: Optimal errors on the imaginary parts of the general HZV couplings at $\sqrt{s} = 250$ GeV.

ϵ_τ	—	0.4	—	—	0.4
ϵ_b	—	—	0.2	—	0.2
$\lvert P \rvert$	—	—	—	0.9	0.9
$\mathrm{Im}\,(b_Z - c_Z)$	.25	.095	.071	.015	.014
$\mathrm{Im}\,(b_\gamma - c_\gamma)$	.055	.027	.023	.018	.018
$\mathrm{Im}\,\tilde{b}_Z$	.049	.018	.014	.0026	.0026
$\mathrm{Im}\,\tilde{b}_\gamma$	.010	.0050	.0043	.0032	.0032

couplings, one can only measure four combinations of their imaginary parts. The other combinations, $\mathrm{Im}\,a_Z$, $\mathrm{Im}\,(b_Z + c_Z)$ and $\mathrm{Im}\,(b_\gamma + c_\gamma)$, only affect the form factor h_1^V, but not h_2^V or h_3^V. They contribute to the amplitudes as a common overall phase, and hence they do not alter the extracted values of $c_i^{(V,A)}$. Thus, these other combinations cannot be measured.

For $\epsilon_\tau = \epsilon_b = P = 0$, the functions $F_i^{(V)}$ with $i = 7, 8, 9$ are suppressed in magnitude by the smallness of A_f and the vanishing of P, while the functions $F_i^{(A)}$ with $i = 7, 8, 9$ have unsuppressed parts. Thus, the errors on $\mathrm{Im}\,(b_\gamma - c_\gamma)$ and $\mathrm{Im}\,\tilde{b}_\gamma$ are much smaller than those on $\mathrm{Im}\,(b_Z - c_Z)$ and $\mathrm{Im}\,\tilde{b}_Z$, respectively, as may be seen in Table 3.

By using any of the three charge and polarization measurements, we gain better sensitivities to the HZZ couplings because the functions $F_i^{(V)}$ with $i = 7, 8, 9$ are less strongly suppressed. The measurement of the tau helicity with 40% efficiency reduces the errors on the HZZ couplings by a factor of about $2/5$. The bottom charge identification with 20% efficiency leads to a reduction by a factor of $2/7$. The electron beam polarization is the most efficient technique for improving the sensitivities. It reduces these errors by a factor of $1/20$. The errors on the $HZ\gamma$ couplings are reduced by a factor of $1/2$ with tau helicity measurements or bottom charge identification, and by a factor of $1/3$ with beam polarization.

For $\epsilon_\tau = \epsilon_b = P = 0$, the errors and the correlation matrix are

$$
\begin{array}{ll}
\begin{array}{ll}
\mathrm{Im}\,(b_Z - c_Z) = 0 \pm .25 \\
\mathrm{Im}\,(b_\gamma - c_\gamma) = 0 \pm .055 \\
\mathrm{Im}\,\tilde{b}_Z \quad\ = 0 \pm .049 \\
\mathrm{Im}\,\tilde{b}_\gamma \quad\ = 0 \pm .010
\end{array}
&
\left(
\begin{array}{cccc}
1 & & & \\
-.94 & 1 & & \\
0 & 0 & 1 & \\
0 & 0 & -.95 & 1
\end{array}
\right) .
\end{array}
\tag{5.19}
$$

There are strong correlations between the errors on the first two terms and those of the latter two. The eigenvectors of the two smallest eigenvalues and their errors read

$$
.20\ \mathrm{Im}\,\tilde{b}_Z + .98\ \mathrm{Im}\,\tilde{b}_\gamma \qquad = 0 \pm .0031, \tag{5.20-a}
$$

$$
.20\ \mathrm{Im}\,(b_Z - c_Z) + .98\ \mathrm{Im}\,(b_\gamma - c_\gamma) = 0 \pm .018. \tag{5.20-b}
$$

For $\epsilon_\tau = 40\%$, $\epsilon_b = 20\%$ and $P = 90\%$, we have

$$
\begin{array}{ll}
\begin{array}{ll}
\mathrm{Im}\,(b_Z - c_Z) = 0 \pm .014 \\
\mathrm{Im}\,(b_\gamma - c_\gamma) = 0 \pm .018 \\
\mathrm{Im}\,\tilde{b}_Z \quad\ = 0 \pm .0026 \\
\mathrm{Im}\,\tilde{b}_\gamma \quad\ = 0 \pm .0032
\end{array}
&
\left(
\begin{array}{cccc}
1 & & & \\
-.10 & 1 & & \\
0 & 0 & 1 & \\
0 & 0 & -.10 & 1
\end{array}
\right) .
\end{array}
\tag{5.21}
$$

The strong correlation between the HZZ and $HZ\gamma$ couplings is lost for the three charge and polarization measurements.

Next, we consider the CM energy $\sqrt{s} = 500$ GeV. For $\epsilon_\tau = 40\%$, $\epsilon_b = 20\%$ and $|P| = 90\%$, we find

$$
\begin{array}{ll}
\begin{array}{ll}
\mathrm{Im}\,(b_Z - c_Z) = 0 \pm .0033 \\
\mathrm{Im}\,(b_\gamma - c_\gamma) = 0 \pm .0037 \\
\mathrm{Im}\,\tilde{b}_Z \quad\ = 0 \pm .0015 \\
\mathrm{Im}\,\tilde{b}_\gamma \quad\ = 0 \pm .0017
\end{array}
&
\left(
\begin{array}{cccc}
1 & & & \\
-.10 & 1 & & \\
0 & 0 & 1 & \\
0 & 0 & -.10 & 1
\end{array}
\right) .
\end{array}
\tag{5.22}
$$

Although the cross section at $\sqrt{s} = 500$ GeV is smaller than the one at $\sqrt{s} = 250$ GeV, the errors on the couplings are reduced because of the s/m_Z^2 factors multiplying the above couplings. The three combinations $\mathrm{Im}\,a_Z$, $\mathrm{Im}\,(b_Z + c_Z)$ and $\mathrm{Im}\,(b_\gamma + c_\gamma)$ cannot be measured even if the CM energy is varied.

6   Conclusion

In the present paper, we have performed a systematic study of the angular distributions of the process $e^+ e^- \to H f \bar{f}$ in order to assess the sensitivities to the seven general HZV couplings by using the optimal-observable method [10, 11, 12, 13]. To that end, we have expanded the differential cross section as a sum of the products of the eighteen model-dependent coefficients $c_i^{(V,A)}$, which contain all the dynamical

information on the HZV couplings, and the corresponding eighteen angular functions $F_i^{(V,A)}$, which depend on the production and decay kinematics, the final-state fermion flavor f, the tau polarization and the electron beam polarization P.

As for the real parts of the HZV couplings, one can only measure six combinations at a given CM energy $\sqrt{s}$. At $\sqrt{s} = 250$ GeV, we gain optimal errors of order 1×10^{-2} (1×10^{-1}) for the HZZ ($HZ\gamma$) couplings assuming $L = 10$ fb^{-1} and $m_H = 120$ GeV. A tau helicity measurement with 40% efficiency reduces the optimal errors on the $HZ\gamma$ couplings to about 2/5 of those obtainable without such a measurement. A bottom charge identification with 20% efficiency reduces these errors to about 2/7 of those with unidentified bottom charge. An electron beam polarization of 90% reduces the optimal errors on the CP-even (CP-odd) $HZ\gamma$ couplings to about 1/20 (1/6) of those with unpolarized beams. The reduction of the errors on the HZZ couplings is at most by 1/2. The sensitivities to the HZV couplings depend on $\sqrt{s}$. The errors on the real parts of the HZV couplings decrease by a factor of about 1/2 to 1/10 when one increases $\sqrt{s}$ from 250 GeV to 500 GeV.

As for the imaginary parts of the HZV couplings, we can only measure four combinations, as long as we only keep terms linear in the couplings. Without the three charge and polarization measurements, we achieve optimal errors of order 1×10^{-2} for Im $\tilde{b}_\gamma$, 5×10^{-2} for Im $(b_\gamma - c_\gamma)$ and Im $\tilde{b}_Z$, and 3×10^{-1} for Im $(b_Z - c_Z)$ with $L = 10$ fb^{-1} at $\sqrt{s} = 250$ GeV. The optimal errors on the HZZ couplings are reduced by factors of about 2/5, 2/7 and 1/20 with the tau helicity measurement, the bottom charge identification and the electron beam polarization, respectively. The errors on the $HZ\gamma$ couplings are at most diminished by a factor of 1/3 with the three charge and polarization measurements. When one increases $\sqrt{s}$ from 250 GeV to 500 GeV, the errors decrease by a factor of 1/2 to 1/5.

In our analysis, we have considered the general HZZ and $HZ\gamma$ interactions. We have neglected the contribution from the dimension-five $HZee$ operator,

$$\frac{1}{m_Z} \sum_{\sigma=\pm} g_\sigma^{HZee} H Z^\mu \bar{e} \gamma_\mu P_\sigma e, \tag{6.1}$$

with $P_\pm = (1 \pm \gamma_5)/2$, which contributes to the cross section at the same order as the operators in the effective Lagrangian (3.1). The simple and very general treatment of the observables in Sect. 4 is no longer valid if the terms in (6.1) are significant. The optimal constraints on the effective couplings can still be obtained by directly studying the g_σ^{HZee} dependences of the differential cross sections. We believe, however, that our approach will be useful in constraining theories that affect the HZV couplings more significantly than the $HZee$ couplings. The contributions from the third-generation squarks in the MSSM [18] provide one an example.

References

[1] J. Nielsen, for the ALEPH Collaboration, Report No. hep-ex/9908016; DELPHI Collaboration, P. Abreu et al., Phys. Lett. B **459** (1999) 367; L3 Collaboration, M. Acciarri et al., Phys. Lett. B **461** (1999) 376; OPAL Collaboration, G. Abbiendi et al., Report No. hep-ex/9908002.

[2] R.L. Kelly, T. Shimada, Phys. Rev. D **23** (1981) 1940; P. Kalyniak, J.N. Ng, P. Zakarauskas, Phys. Rev. D **29** (1984) 502.

[3] J.C. Romão, A. Barroso, Phys. Lett. B **185** (1987) 195.

[4] J. Fleischer, F. Jegerlehner, Nucl. Phys. B **216** (1983) 469; S. Dawson, H.E. Haber, Phys. Rev. D **44** (1991) 53; B.A. Kniehl, Z. Phys. C **55** (1992) 605; A. Denner, J. Küblbeck, R. Mertig, M. Böhm, Z. Phys. C **56** (1992) 261.

[5] B.A. Kniehl, Phys. Rep. **240** (1994) 211.

[6] R.M. Godbole, P. Roy, Phys. Rev. Lett. **50** (1983) 717.

[7] R. Rattazzi, Z. Phys. C **40** (1988) 605.

[8] K. Hagiwara, M.L. Stong, Z. Phys. C **62** (1994) 99.

[9] V. Barger, K. Cheung, A. Djouadi, B.A. Kniehl, P.M. Zerwas, Phys. Rev. D **49** (1994) 79.

[10] D. Atwood, A. Soni, Phys. Rev. D **45** (1992) 2405.

[11] M. Davier, L. Duflot, F. Le Diberder, A. Rougé, Phys. Lett. B **306** (1993) 411.

[12] M. Diehl, O. Nachtmann, Z. Phys. C **62** (1994) 397.

[13] J.F. Gunion, B. Grzadkowski, X.-G. He, Phys. Rev. Lett. **77** (1996) 5172.

[14] K. Hagiwara, R.D. Peccei, D. Zeppenfeld, K. Hikasa, Nucl. Phys. B **282** (1987) 253.

[15] Particle Data Group, C. Caso et al., Eur. Phys. J. C **3** (1998) 1.

[16] S. Eidelman, F. Jegerlehner, Z. Phys. C **67** (1995) 585; H. Burkhardt, B. Pietrzyk, Phys. Lett. B **356** (1995) 398.

[17] J.H. Kühn, Phys. Rev. D **52** (1995) 3128.

[18] A. Pilaftsis, C.E.M. Wagner, Nucl. Phys. B **553** (1999) 3.

Figure captions

Figure 1: General HZV coupling. The arrows indicate the direction of the four-momentum flow.

Figure 2: Contours of $\chi^2 = 1$ in the (b_γ, c_γ) plane for $\sqrt{s} = 250$ GeV. The other degrees of general couplings are integrated out. The central values of b_γ and c_γ are assumed to coincide with their SM values, $b_\gamma = c_\gamma = 0$. The errors are estimated by means of the optimal-observable method under the following four conditions: (a) $\epsilon_\tau = \epsilon_b = P = 0$; (b) $\epsilon_\tau = 0.4$ and $\epsilon_b = P = 0$; (c) $\epsilon_b = 0.2$ and $\epsilon_\tau = P = 0$; or (d) $\epsilon_\tau = 0.4$, $\epsilon_b = 0.2$ and $|P| = 0.9$.

Figure 3: Contours of $\chi^2 = 1$ in the (b_Z, c_Z) plane for $\sqrt{s} = 250$ GeV. $a_Z = 0$ and the other degrees of general couplings are integrated out. The central values of b_Z and c_Z are assumed to coincide with their SM values, $b_Z = c_Z = 0$.

Figure 4: Contours of $\chi^2 = 1$ in the $(\tilde{b}_Z, \tilde{b}_\gamma)$ plane for $\sqrt{s} = 250$ GeV. The other degrees of general couplings are integrated out. The central values of $\tilde{b}_Z$ and $\tilde{b}_\gamma$ are assumed to coincide with their SM values, $\tilde{b}_Z = \tilde{b}_\gamma = 0$.

Figure 5: The projections of the $\chi^2 = 1$ contours onto the (a_Z, b_Z), (b_Z, c_Z) and (c_Z, a_Z) planes for $\sqrt{s} = 250$ GeV and 500 GeV. The central values of a_Z, b_Z and c_Z are assumed to coincide with their SM values, $a_Z = b_Z = c_Z = 0$. The errors are estimated under the condition $\epsilon_\tau = 0.4$, $\epsilon_b = 0.2$ and $|P| = 0.9$. Dashed (thin solid) lines represent the one-σ contours obtained at $\sqrt{s} = 250$ (500) GeV. Thick solid curves represent the combined one-σ contours.

$$i\Gamma^V_{\alpha\beta} = i g_Z m_Z \left[h_1^V g_{\alpha\beta} + \frac{h_2^V}{m_Z^2} q_\alpha p_{Z\beta} + \frac{h_3^V}{m_Z^2} \epsilon_{\alpha\beta\mu\rho} q^\mu p_Z^\rho \right]$$
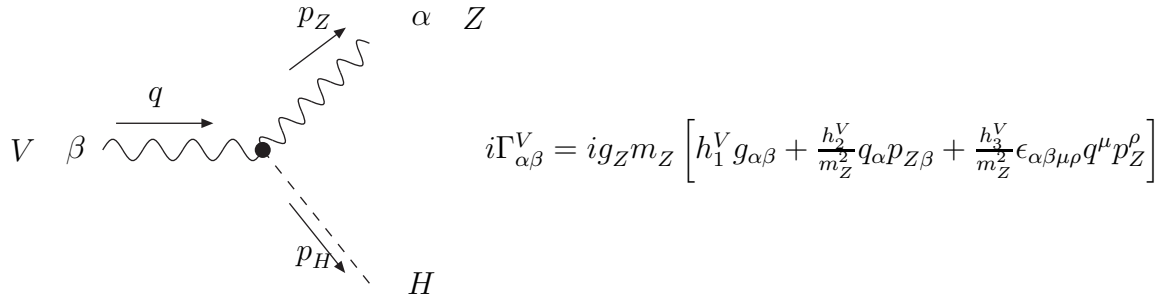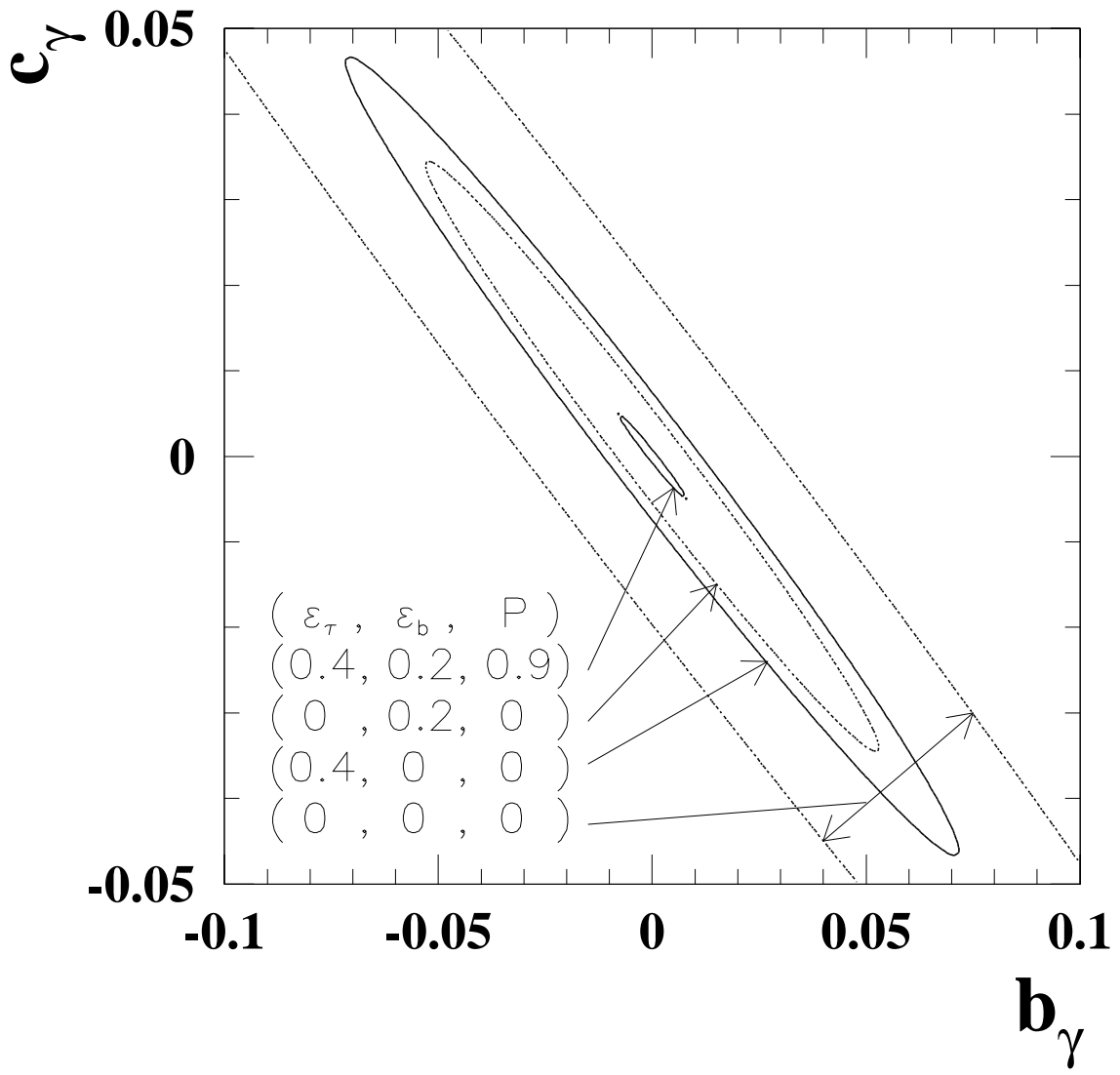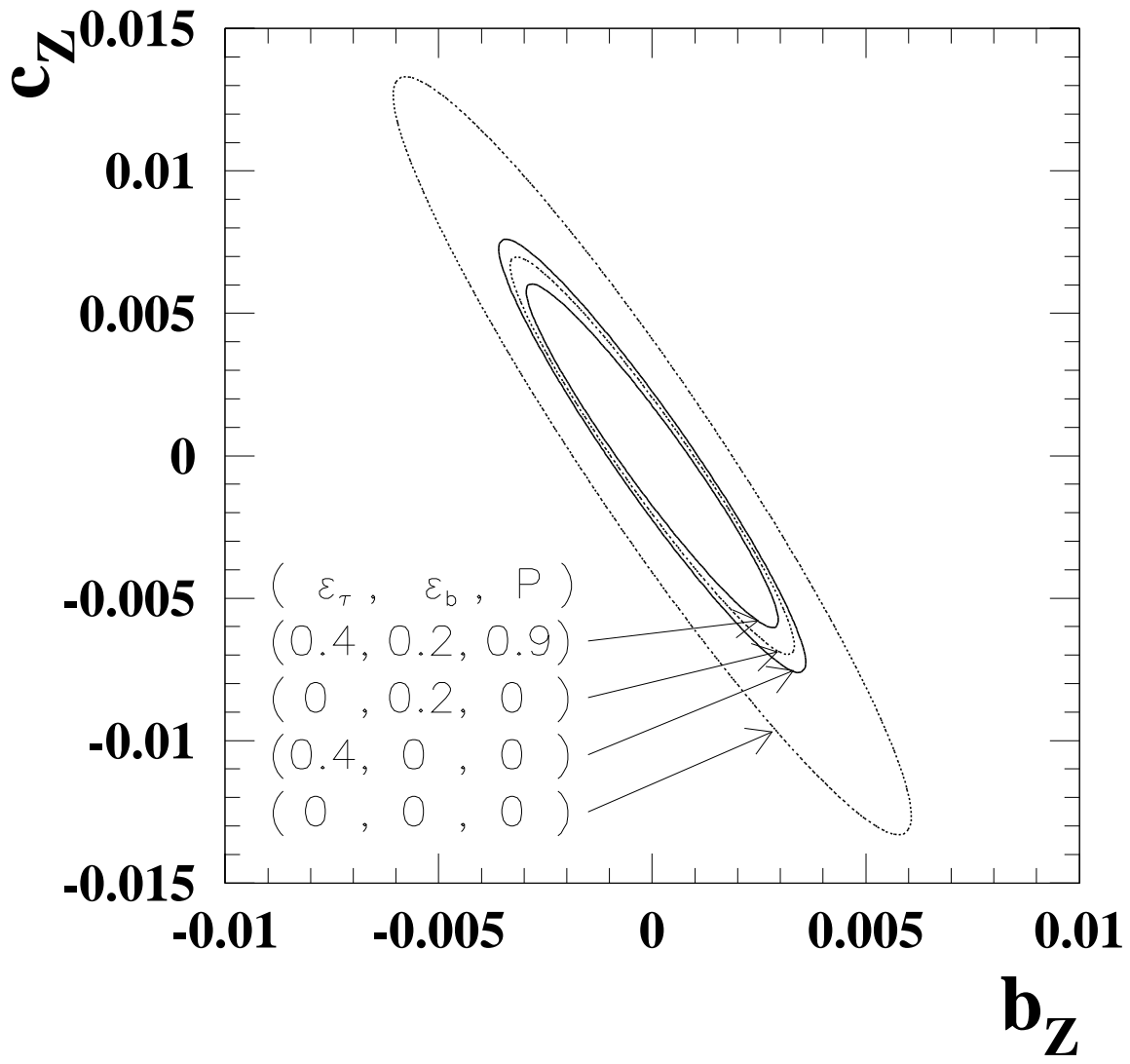
Figure 1:

Figure 2:

Figure 3:

Figure 4:

Figure 5: